Journal of Sound and Vibration 329 (2010) 2435–2449

Contents lists available at ScienceDirect

Journal of Sound and Vibration

journal homepage: www.elsevier.com/locate/jsvi

On the efficacy of an inertial active device with internal time-delayed feedback for controlling self-excited oscillations

S. Chatterjee *, A.K. Mandal

Department of Mechanical Engineering, Bengal Engineering and Science University, Shibpur, Howrah 711 103, West Bengal, India

ARTICLE INFO

Article history:
Received 27 July 2009
Received in revised form
23 November 2009
Accepted 25 November 2009
Handling Editor: J. Lam
Available online 29 January 2010

ABSTRACT

An inertial, active device running on its internal feedback is proposed for controlling the self-excited vibration of a single degree-of-freedom Rayleigh oscillator. The control strategy utilizes the time-delayed feedback of the acceleration of the sprung mass of the device. The feedback law is recursive in nature and based on large amount of weighted information regarding the past history of the dynamics. The proposed device, when properly tuned, either completely quenches or reduces the amplitude of vibration. A comparison with a passive absorber reveals that the proposed active absorber can achieve better stability conditions. However like a passive absorber, the device has finite robustness, i.e., it can control only a certain level of instability inherent in the primary self-excited system.

1. Introduction

There are numerous examples of self-excited vibration like, flutter of aircraft wings and turbine blades, instability of rotating shafts, friction-induced vibrations in brakes and clutches, galloping of transmission lines, flow induced vibration in pipes, aerodynamically induced motion in bridges, chattering of machine tools etc. The mechanism of self-excited vibration is attributed to the presence of a nonlinear state dependent force inherent in the system dynamics, where the dynamics in the phase-space around the unstable static equilibrium is governed by an equivalent negative damping force and the dynamics far away from the equilibrium is positively damped. As a result of these two opposing forces, a steady-state vibration is produced. The most commonly studied mathematical models of self-excited oscillators are the van der Pol oscillator and the Rayleigh oscillator.

In most cases, self-excited vibration poses a great problem in the safe running of engineering systems and devices. Therefore, it is necessary to find means of either completely suppressing the vibration, wherever possible, or reducing the amplitude of vibration. In principle, self-excited vibration can be controlled by increasing the overall damping of the vibrating body. Several passive and active methods can be employed for enhancing the level of damping of the structure.

The most intuitive passive control device is the conventional dynamic vibration absorber (DVA). However, the DVA becomes effective only for larger mass ratio of the absorber [1,2]. Sometimes, this requirement may render the DVA rather infeasible in suppressing self-excited oscillations. Moreover, an appropriate tuning of the absorber frequency is also necessary for the successful operation of the DVA. Asfar [3] has shown that use of the Lanchester damper can circumvent the requirement of the absorber tuning. Use of an appropriately designed impact damper is another alternative [4]. Tondl et al. [5] have also discussed the use of autoparametric absorber for controlling self-excited oscillations.

* Corresponding author.
E-mail address: shy@mech.becs.ac.in (S. Chatterjee).

0022-460X/$ - see front matter © 2010 Elsevier Ltd. All rights reserved.
doi:10.1016/j.jsv.2009.11.028

Active control methods are more attractive and versatile compared to passive vibration control techniques. Several active control methods for suppressing self-excited oscillations have been reported. Hall et al. [6] have proposed a new strategy, based on the nonlinear phenomenon of saturation for controlling the self-excited, aerodynamic flutter of a wing. The saturation controller can effectively suppress flutter oscillations of a wing when the controller frequency is actively tuned. El-Badawy and Nasar El-Deen [7] have also demonstrated the feasibility of the nonlinear saturation based control to suppress self-excited vibrations by using an active nonlinear feedback control. The authors use the van der Pol oscillator as the working model for a self-excited system. A saturation phenomenon is induced by tuning the frequency of an under-damped second-order absorber to one-half that of the primary system. Tondl [8,9] proposes a new concept of suppressing self-excited vibrations using parametric excitation. It is shown that within a certain frequency interval, a phenomenon called 'parametric antiresonance' can occur and self-excited vibrations can be fully cancelled by the parametric excitation. Subsequently several researchers have further investigated and applied this concept for suppressing self-excited vibrations of different real-life systems [10–15]. Chatterjee [16] proposes a novel active, model-independent method of controlling vibrations using impulses generated by alternately contacting and expanding a mass-loaded, piezoelectric stack actuator. The above concept is adapted from the working principle of an impact damper. The proposed method can control any type of the vibration including self-excited vibration.

Friction driven self-excited oscillation is another class of significant problem which has been addressed several times in the literature. Several active and semi-active methods have been proposed to control friction-induced oscillations [17–23].

Despite the number of advantages, the performance of a closed-loop control system may significantly deteriorate owing to the unavoidable time-delay present in the digital feedback circuit. To circumvent this problem, researchers have proposed using intentional and controllable time-delay in the feedback circuit. This particular method, termed as the time-delayed feedback control, has emerged as an efficient control technique in modern control strategies. Proper choices of the time-delay and the control gain in the feedback circuit ensure the stability of the static equilibrium. Time-delayed feedback has been proven effective in controlling different kinds of vibrations including self-excited vibrations. Atay [24,25], Maccari [26,27] and Li et al. [28] discuss the use of time-delayed state feedback method in controlling free, forced and parametric vibrations of the Van der Pol oscillator. Elmer [29] proposes a method of controlling friction-induced oscillations by normal load modulation based on the time-delayed state feedback. Das and Mallik [30] consider the time-delayed PD feedback control of the forced vibration of a friction-driven system. Chatterjee [31] has discussed the time-delayed feedback control of different types of friction-induced instabilities and oscillations. Chatterjee and Mahata [32] have proposed active absorbers operating on time-delayed feedback for suppressing friction-induced self-excited vibration.

The present paper proposes a class of inertial, vibration control device that when attached to the vibrating body will operate actively without any sensory feedback from the primary vibrating structure. The appended, active device will run on the feedback, internal to the device itself. Fundamentally, the proposed device comprises of a spring mass system attached to a rigid base and an actuator placed in between the base and the mass. The actuator is controlled by a sensory feedback of the oscillating mass of the device itself. The base of the device can be simply connected to the primary structure to produce either complete stabilization or reduction of the intensity of the self-excited vibration.

An appropriate choice of the sensor for practical applications is always difficult. For example, though theoretically the state-variable feedback is the most common and robust control method, difficulty in measuring the displacement and velocity directly without an inertial reference frame renders the practical implementation of the state feedback method often infeasible. However, direct measurement of the acceleration using an accelerometer is a cheap and reliable alternative. Using double integration of the acceleration signal for the indirect displacement measurement often produces large error; so is true for the velocity measurement. However, introducing a phase change in the acceleration feedback signal can produce the desired damping effect. Introducing a controllable time-delay in the feedback path is one of the many ways of producing this phase change. The present paper considers the time-delayed acceleration of the vibrating mass of the active device as the sensory feedback for controlling the actuator.

A mathematical model of the system consisting of a single degree-of-freedom self-excited Rayleigh oscillator attached with the above-mentioned active device is developed. Both linear and nonlinear stability analyses are performed to understand the dynamics of the system. In order to assess the efficacy of the proposed device, its optimal performance is compared with that of the passive DVA. The device is shown to perform better compared to the passive DVA.

2. Mathematical model

A mathematical model of the system attached with the active device is illustrated in Fig. 1. The primary structure is a single degree-of-freedom self-excited Rayleigh oscillator having the primary mass M suspended by a spring of stiffness K. A secondary mass m is attached to the primary structure by a spring of stiffness K_a. An actuator is placed in between the primary and the secondary mass to apply the control force F_c. X and Y are the absolute displacements of the primary and the secondary mass, respectively.

Equations of motion of the two degrees-of-freedom system illustrated in Fig. 1 read as

$$MX'' + F(X') + KX + K_a(X-Y) = -F_c, \tag{1}$$

$$mY'' + K_a(Y-X) = F_c, \tag{2}$$

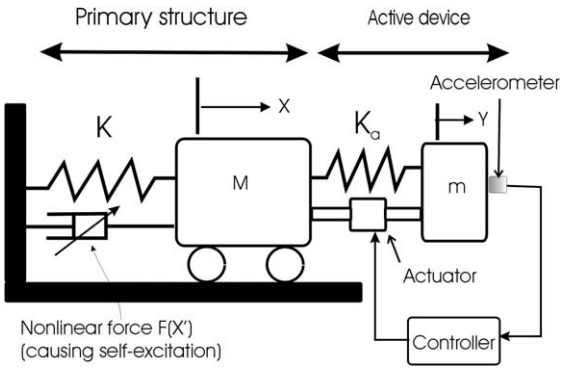

Fig. 1. Mathematical model of the system.

where the nonlinear force $F(X')$, responsible for the self-excitation is expressed as

$$F(X') = aX' + bX'^3, \quad a < 0, b > 0. \tag{3}$$

The 'dash' denotes the derivative with respect to time t^* in Eqs. (1)–(3).

The control force (F_c) is expressed as

$$F_c = K_c U, \tag{4}$$

where K_c is the control gain.

The control signal U is synthesized as the recursive weighted summation of the acceleration of the secondary mass and the control signal itself both at a specific time-delay τ^*. The control signal is mathematically represented as

$$U = Y''(t^* - \tau^*) + RU(t^* - \tau^*), \tag{5}$$

where τ^* is the time-delay and R is the weighting factor, henceforth termed as the *recursive gain*. The absolute numerical value of the parameter R is less than unity. Thus, the control can be rightly termed as the recursive time-delayed feedback control [33].

An alternative mathematical representation of the control signal given in (5) is as follows

$$U = \sum_{k=1}^{\infty} R^{k-1} Y''(t^* - k\tau^*). \tag{6}$$

Though the particular mathematical form of the control signal expressed in Eq. (5) is convenient for practical realization of the control, Eq. (6) offers a better interpretation of the control action. One can interpret the control signal in Eq. (5) as the infinite weighted sum of the acceleration of the secondary mass measured at equal intervals in the past. Evidently, a higher weight is given to a more recent data. Thus, the feedback signal uses a large amount of information about the past history of the dynamics. It is interesting to note that the control law defined in Eqs. (4)–(6) is the generalized form of the time-delayed acceleration feedback, whence one gets the ordinary time-delayed acceleration feedback, as a special case, for $R=0$ (non-recursive feedback). The advantage of such a feedback is discussed elsewhere in the paper.

Eqs. (1) and (2) can be recast in the following non-dimensional form:

$$\begin{bmatrix} 1 & 0 \\ 0 & \mu \end{bmatrix} \begin{Bmatrix} \ddot{x} \\ \ddot{y} \end{Bmatrix} + \begin{bmatrix} 1+\mu\omega_a^2 & -\mu\omega_a^2 \\ -\mu\omega_a^2 & \mu\omega_a^2 \end{bmatrix} \begin{Bmatrix} x \\ y \end{Bmatrix} = \begin{Bmatrix} -f(\dot{x}) \\ 0 \end{Bmatrix} + \begin{Bmatrix} -f_c \\ f_c \end{Bmatrix}, \tag{7}$$

with the following non-dimensional quantities:

$$x = \frac{X}{x_0}, y = \frac{Y}{x_0}, \quad \mu = \frac{m}{M}, \quad \omega_a = \frac{\omega_a^*}{\omega_0},$$

where x_0 is an arbitrary length (may be taken as the static deflection of the primary oscillator), $\omega_0 = \sqrt{K/M}$ is the natural frequency of the primary system and $\omega_a^* = \sqrt{K_a/m}$ is the natural frequency of the absorber.

The 'dot' denotes the differentiation with respect to the non-dimensional time $t = \omega_0 t^*$.

Accordingly, the nonlinear self-exciting force in Eq. (3) is expressed in the non-dimensional form as

$$f(\dot{x}) = \alpha\dot{x} + \beta\dot{x}^3, \quad \alpha < 0, \beta > 0, \tag{8}$$

where $\alpha = a/M\omega_0$, $\beta = b\omega_0 x_0^2/M$ are the two non-dimensional quantities.

The non-dimensional representation of the control force defined in Eqs. (4) and (5) is given as

$$f_c = -k_c u, \tag{9}$$

with

$$u = \ddot{y}(t-\tau) + Ru(t-\tau), \tag{10}$$

where the non-dimensional control gain is $k_c = K_c/M$ and the non-dimensional time-delay is $\tau = \omega_0 \tau^*$.

An alternative expression of Eq. (10) in the non-dimensional form is obtained from Eq. (6) as

$$u = \sum_{k=1}^{\infty} R^{k-1} \ddot{y}(t-k\tau). \tag{11}$$

3. Stability of the equilibrium with the passive absorber

In order to show the worth of the proposed active device, it will be pertinent to compare its performance with that of the passive DVA. Before analysing the performance of the proposed active device in the subsequent sections, a brief discussion on the performance of the passive DVA is presented in this section. Further details about the performance of the DVA may be found in [2]. The mathematical model of the self-excited oscillator, with a passive DVA attached, may be obtained by using the following expression of the control force in Eq. (7):

$$f_c = c(\dot{x} - \dot{y}), \tag{12}$$

where c is the non-dimensional viscous damping coefficient of the DVA.

The characteristic equation of the system with the DVA is a fourth-order polynomial equation given below

$$s^4 + c_3 s^3 + c_2 s^2 + c_1 s + c_0 = 0, \tag{13}$$

where $c_3 = c + \alpha + c/\mu$, $c_2 = 1 + \omega_a^2 + \mu\omega_a^2 + \alpha c/\mu$, $c_1 = \alpha\omega_a^2 + c/\mu$, and $c_0 = \omega_a^2$.

The regions of stability of the static equilibrium are shown in Fig. 2. It is observed that the stability cannot be achieved beyond a critical value of α. It may be noted that the degree of instability inherent in the original self-excited system is quantified by the value of the negative damping (α) in the system. Clearly the more negative is the value of α, the stronger

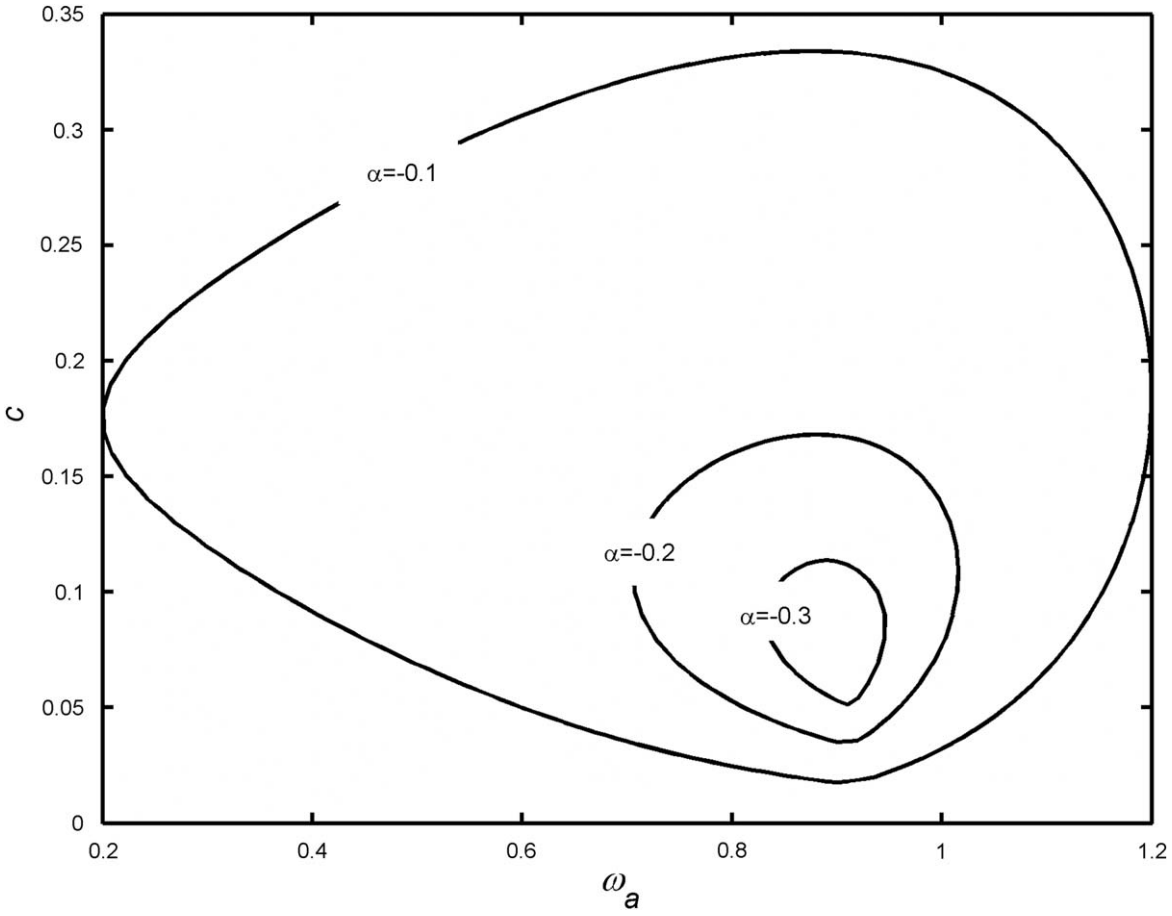

Fig. 2. Regions of stability of the static equilibrium with the passive DVA. μ=0.2.

is the instability. It is important to obtain the optimum values of the absorber damping and the frequency. There may be two bases for the optimum selection of the absorber parameters. One may attempt to maximize either the robustness or some measure of the stability of the designed system. Towards this end, the following two definitions are introduced below:

Definition 1. *Robustness*—The absolute value of the maximum instability inherent to the original self-excited oscillator that can be stabilized by the DVA is defined as the robustness of the system.

Definition 2. *σ-stability*—Value of the real part of the dominant, stable (lying in left hand *s*-plane) eigenvalues of the linearized system. The more negative is this value, the higher is the σ-stability.

According to the Definition 1, the passive DVA has only finite robustness. Indeed, the robustness can be improved further by using larger mass ratios (results are not shown). However, using a large mass ratio is somewhat impractical. It is also observed from the stability plots that the value of the absorber frequency giving the maximum robustness is little lower than the frequency of oscillation of the self-excited system without the absorber and decreases with the increasing mass ratio.

A typical σ-stability map of the system with the DVA is shown in Fig. 3. Using the Definition 2, the real parts of the dominant roots of the characteristic Eq. (13) are mapped in the plane of the absorber damping vs. absorber frequency. The absorber parameters selected inside the darker region apparently gives a better σ-stability. Numerical values of the maximum σ-stability and the corresponding optimum absorber parameters are listed in Table 1 for different values of the negative damping parameter α. It is rather counterintuitive to observe that the optimum damping decreases with the increasing degree of instability inherent to the self-excited system. However, the σ-stability decreases and the required absorber frequency increases with the increasing value of α.

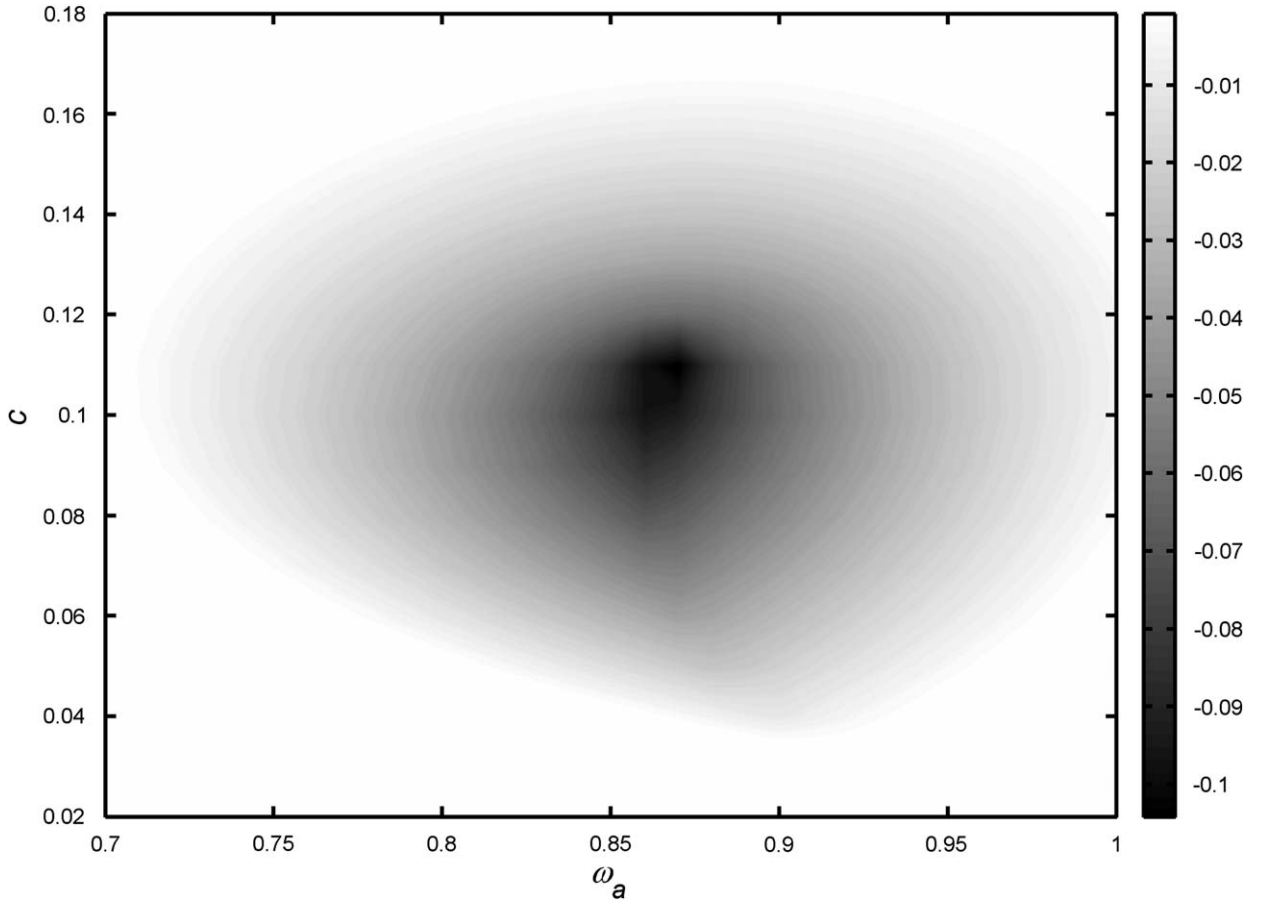

Fig. 3. σ-stability map for the passive absorber. μ=0.2, α= −0.2.

Table 1
Optimum parameter values of the passive absorber (μ=0.2).

α	Maximum σ-stability	Optimum absorber frequency	Optimum damping
−0.1	−0.1481	0.85	0.12
−0.2	−0.1048	0.87	0.11
−0.3	−0.0531	0.89	0.09
−0.4	−0.0109	0.9	0.08

4. Linear stability of the static equilibrium with the active absorber

For analysing the local stability of the trivial equilibrium of the system, Eq. (7) is linearized about its equilibrium. The Laplace transform of the linearized equations yields the following quasi-polynomial characteristic equation:

$$P(s)-Q(s)e^{-s\tau}=0, \tag{14}$$

where

$$P(s)=\mu s^4+\alpha\mu s^3+\chi s^2+\alpha\mu\omega_a^2 s+\mu\omega_a^2, \tag{15}$$

and

$$Q(s)=(\mu R-k_c)s^4+\alpha(\mu R-k_c)s^3+(\chi R-k_c)s^2+\alpha\mu\omega_a^2 Rs+\mu\omega_a^2 R=0, \tag{16}$$

with $\chi=\mu+\mu\omega_a^2+\mu^2\omega_a^2$.

The roots of Eq. (14) are purely imaginary on the root-switching boundaries where a pair of complex conjugate roots of the characteristic equation migrate from the left hand to the right hand side of the s-plane or vice versa. Substituting $s=j\omega$ into Eq. (14) and separating the real and imaginary parts, yields

$$\cos(\omega\tau)=\frac{A_0D_0+B_0C_0}{C_0^0+D_0^2}, \tag{17}$$

$$\sin(\omega\tau)=\frac{B_0D_0-A_0C_0}{C_0^0+D_0^2}, \tag{18}$$

where $A_0=\mu\omega^4-\chi\omega^2+\mu\omega_a^2$, $B_0=\alpha\mu\omega(\omega^2-\omega_a^2)$, $C_0=\alpha(\mu R-k_c)\omega^3-\alpha\mu\omega R\omega_a^2$, and $D_0=(\mu R-k_c)\omega^4-(\chi R-k_c)\omega^2+\mu R\omega_a^2$.

Eliminating τ from Eqs. (17) and (18), yields the following polynomial equation of ω:

$$(A_0D_0+B_0C_0)^2+(B_0D_0+A_0C_0)^2-(C_0^2+D_0^2)^2=0. \tag{19}$$

The critical frequency ω_c is obtained by solving the above frequency equation (Eq. (19)) and the corresponding critical time-delay is computed as

$$\tau_c=\frac{1}{\omega_c}\left[\tan^{-1}\left(\frac{B_0D_0-A_0C_0}{A_0D_0+B_0C_0}\right)+2n\pi\right], n=1,2,\ldots \tag{20}$$

Thus, for the stability of the equilibrium to switch at the critical values computed above, the eigenvalues must cross the imaginary axis from the left half to the right half of the s-plane or the vice versa. This is possible when the speed of the crossing with respect to the increasing value of the time-delay is non-trivial. The speed of the eigenvalue crossing on a switching boundary is expressed as

$$V(\omega_c,\tau_c)=\mathrm{sign}\left[\mathrm{Re}\left(\frac{ds}{d\tau}\Big|_{s=j\omega_c,\tau=\tau_c}\right)\right], \tag{21}$$

where

$$\frac{ds}{d\tau}=\frac{s}{\left(\frac{1}{Q}\frac{dQ}{ds}-\frac{1}{P}\frac{dP}{ds}-\tau\right)}. \tag{22}$$

A pair of complex conjugate eigenvalues with positive real parts crosses the imaginary axis form right hand s-plane to left hand s-plane when τ increases past τ_c across a stability switch boundary with $V<0$. Just the opposite thing happens when the switch boundary is crossed with $V>0$. Since V=0 signifies the non-crossing of the imaginary axis by the eigenvalues, the corresponding critical values must be neglected for the computation of the stability boundaries. It is noted that the uncontrolled system (for the range of parameter values chosen) has two pairs of complex conjugate eigenvalues with positive real parts. Therefore, two consecutive crossings of the switch boundary with $V<0$ are required for the stability of the static equilibrium of the controlled system.

Before proceeding further, it may be noted the system under consideration is a neutral time-delayed system [34]. Therefore, it is important to know the behaviour of the non-system poles as τ goes from 0 to 0^+. This is checked by the

continuity of the roots of the characteristic equation at $\tau=0$. For the present problem, the root continuity at $\tau=0$ is guaranteed if the roots of the following equation, obtained from Eq. (14), lie in the left hand side of the s-plane:

$$\mu-(\mu R-k_c)e^{-s\tau}=0. \tag{23}$$

It is not difficult to show that all roots the system (23) lie in the left hand s-plane if

$$\left|R-\frac{k_c}{\mu}\right|<1. \tag{24}$$

Eq. (24) gives a necessary delay-free condition of the stability. When the condition (24) is violated, the system has an infinite number of unstable poles at $\tau=0^+$. However, within the range of the gains as prescribed by the condition (24), the number of unstable pair of complex poles at $\tau=0^+$ is two.

Using Eqs. (19)–(24), the local stability boundaries are plotted in the plane of the control gain vs. time-delay for a chosen value of the absorber frequency as shown in Figs. 4(a) and (b). It is observed that the proposed active device can stabilize the static equilibrium up to a certain level of the inherent instability quantified by the value of α. The stability plots in the plane of the control gain vs. absorber frequency are illustrated in Fig. 5, which demonstrates that the absorber must be appropriately tuned to achieve the stability. For the stability, the frequency of the active absorber, like the passive absorber, should lie closer to the frequency of self-oscillation without the active device attached. Fig. 6 shows the effect of the recursive gain on the stability. Further discussions on the effect of the recursive gain are available in the next section.

5. Active vs. passive absorber

At this point it is pertinent to compare the performance of the passive absorber (discussed in Section 3) with that of the proposed active device. From the local stability analysis it is observed that the maximum robustness achieved by the proposed active device closely compares with that obtained by a passive absorber. In fact, the active device is slightly more robust. For estimating the σ-stability, the dominant roots of the characteristic equation (Eq. (14)) of the system are computed using the *quasi-polynomial mapping algorithm* [35]. The maximum σ-stability of the system with the active absorber and the corresponding optimal values of the gain and the time-delay are listed in Tables 2 and 3. Apparently, the σ-stability improves a lot due to the recursive feedback, particularly for lower values of α. For example, with $\alpha=-0.2$ and $\mu=0.2$ the maximum σ-stability achieved by the passive absorber is -0.1048 (see Table 1). However, with the active device, the maximum σ-stability can be as high as -0.1766 (with the absorber frequency $\omega_a=0.85$ and the recursive gain $R=0.4$); i.e., a 68.51 percent improvement in the σ-stability is achieved using the active device.

In order to further substantiate the above conclusion that the proposed active device can achieve better σ-stability, numerical simulations of the systems are carried out. Towards this end, MATLAB SIMULINK models are developed. All simulations are run from the initial conditions [1, 0, 0, 0], i.e. with the primary mass initially displaced by unity. The optimum parameter values of the passive and the active absorber are taken from Tables 1 and 3, respectively.

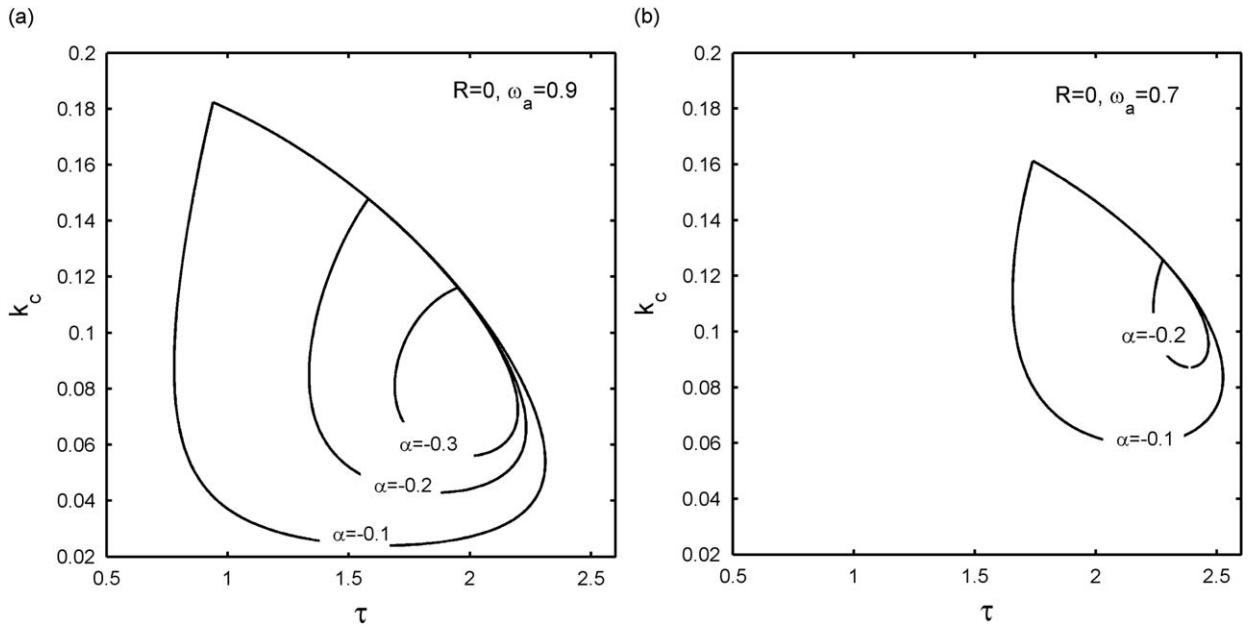

Fig. 4. Local stability regions in the gain vs. time-delay plane. $\mu=0.2$.

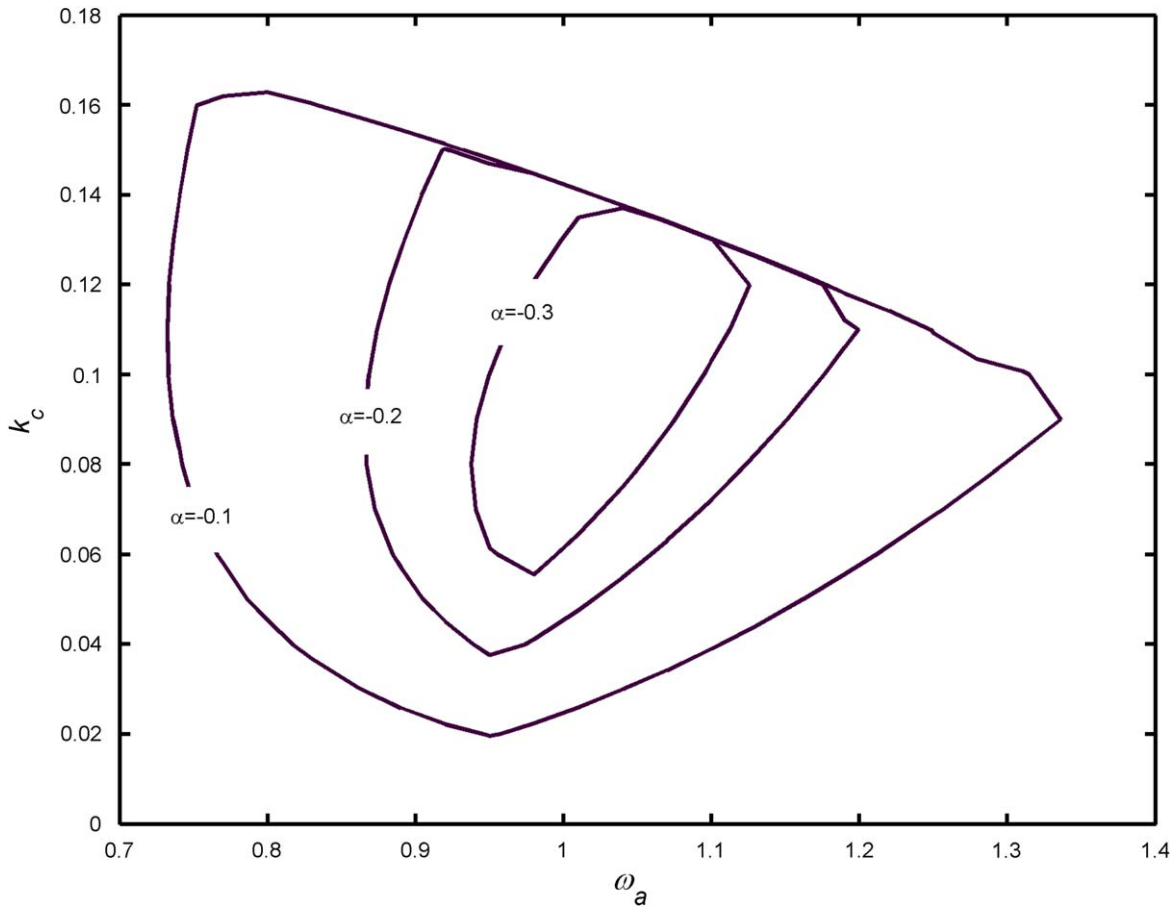

Fig. 5. Local stability regions in the gain vs. absorber frequency plane. τ=1.5, μ=0.2.

The corresponding results are plotted in Figs. 7(a)–(c). From these figures it is evident that the active device produces better transient response (i.e., higher σ-stability) compared to the optimal passive absorber.

6. Nonlinear analysis

The linearized stability analysis presented in Section 4 gives an idea about the local stability of the static equilibrium. In this section, the multiple time scale (MTS) analysis is employed to gain a deeper insight into the global nonlinear dynamics of the system with the active device attached. To make the system amenable to the MTS analysis, both the self-excitation and the control are assumed as weak forces. Under these circumstances, one rewrites the non-dimensional Eq. (7) as

$$[M]\begin{Bmatrix}\ddot{x}\\ \ddot{y}\end{Bmatrix}+[K]\begin{Bmatrix}x\\ y\end{Bmatrix}=\varepsilon\begin{Bmatrix}f_1\\ f_2\end{Bmatrix} \tag{25}$$

where $\varepsilon \ll 1$ is a small positive quantity, $f_1=-(\alpha^*\dot{x}+\beta^*\dot{x}^3)+k_c^*u$, $f_2=-k_c^*u$, with $\varepsilon k_c^*=k_c$, $\varepsilon\alpha^*=\alpha$, $\varepsilon\beta^*=\beta$.

The following similarity transformation is used for the pseudo-normalization of Eq. (25):

$$\begin{Bmatrix}x\\ y\end{Bmatrix}=[\Phi]\begin{Bmatrix}z\\ v\end{Bmatrix}, \tag{26}$$

where

$$[\Phi]=\begin{bmatrix}1 & 1\\ \lambda_1 & \lambda_2\end{bmatrix},$$

and $\lambda_i=1+\mu\omega_a^2-\omega_i^2/\mu\omega_a^2$, i=1,2 with ω_i as the natural frequency of the undamped, uncontrolled system.

Following the pseudo-normalization, Eq. (25) is transformed into

$$\begin{bmatrix}1 & 0\\ 0 & 1\end{bmatrix}\begin{Bmatrix}\ddot{z}\\ \ddot{v}\end{Bmatrix}+\begin{bmatrix}\omega_1^2 & 0\\ 0 & \omega_2^2\end{bmatrix}\begin{Bmatrix}z\\ v\end{Bmatrix}=\varepsilon\begin{bmatrix}\dfrac{-\lambda_2}{\lambda_1-\lambda_2} & \dfrac{1}{\mu(\lambda_1-\lambda_2)}\\ \dfrac{\lambda_1}{\lambda_1-\lambda_2} & \dfrac{-1}{\mu(\lambda_1-\lambda_2)}\end{bmatrix}\begin{Bmatrix}f_1\\ f_2\end{Bmatrix}. \tag{27}$$

The two time scale expansion of the solution of Eq. (27) is written as

$$z=z_0(T_0,T_1)+\varepsilon z_1(T_0,T_1), \tag{28}$$

$$v=v_0(T_0,T_1)+\varepsilon v_1(T_0,T_1), \tag{29}$$

where the two time scales for the expansion are $T_0=t$ and $T_1=\varepsilon t$.

Using (28) and (29) in Eq. (27) and coining the terms of different orders, one obtains

$$\varepsilon^0:\ D_0^2z_0+\omega_1^2z_0=0, \tag{30}$$

$$\varepsilon^1:\ D_0^2z_1+\omega_1^2z_1=-2D_1D_0z_0+\frac{\lambda_2}{\lambda_1-\lambda_2}g_1-\frac{1}{\lambda_1-\lambda_2}\left(\lambda_2+\frac{1}{\mu}\right)g_2, \tag{31}$$

$$\varepsilon^0:\ D_0^2v_0+\omega_1^2v_0=0, \tag{32}$$

$$\varepsilon^1:\ D_0^2v_1+\omega_1^2v_1=-2D_1D_0v_0-\frac{\lambda_1}{\lambda_1-\lambda_2}g_1+\frac{1}{\lambda_1-\lambda_2}\left(\lambda_1+\frac{1}{\mu}\right)g_2, \tag{33}$$

where $D_0=\partial/\partial T_0$, $D_1D_0=\partial^2/\partial T_1\partial T_0$, $D_0^2=\partial^2/\partial T_0^2$, $g_1=\alpha^*D_0(z_0+v_0)+\beta^*\{D_0(z_0+v_0)\}^3$, and $g_2=k_c^*\sum_{k=1}^{\infty}R^{k-1}\{\lambda_1D_0^2z_0(T_0-k\tau)+\lambda_2D_0^2v_0(T_0-k\tau)\}$.

The solutions of equations (30) and (32) are, respectively,

$$z_0=A\cos(\omega_1T_0+\theta), \tag{34}$$

$$v_0=B\cos(\omega_2T_0+\phi) \tag{35}$$

Substituting (34) into Eq. (31) and (35) into Eq. (33) and subsequently removing the secular terms, yields the following amplitude and phase equations:

$$\frac{\partial A}{\partial T_1}=\frac{A}{2}\left[\frac{\lambda_2}{\lambda_1-\lambda_2}\left\{\alpha^*+\frac{3}{4}\beta^*(A^2\omega_1^2+2B^2\omega_2^2)\right\}-\frac{\lambda_1\omega_1}{\lambda_1-\lambda_2}\left(\lambda_2+\frac{1}{\mu}\right)k_c^*S_1(R,\tau)\right], \tag{36}$$

$$\frac{\partial B}{\partial T_1}=\frac{B}{2}\left[\frac{-\lambda_1}{\lambda_1-\lambda_2}\left\{\alpha^*+\frac{3}{4}\beta^*(B^2\omega_2^2+2A^2\omega_1^2)\right\}+\frac{\lambda_2\omega_2}{\lambda_1-\lambda_2}\left(\lambda_1+\frac{1}{\mu}\right)k_c^*S_2(R,\tau)\right], \tag{37}$$

$$\frac{\partial\theta}{\partial T_1}=-\frac{1}{2}\left(\frac{\lambda_1\omega_1}{\lambda_1-\lambda_2}\right)\left(\lambda_2+\frac{1}{\mu}\right)k_c^*C_1(R,\tau), \tag{38}$$

$$\frac{\partial\phi}{\partial T_1}=\frac{1}{2}\left(\frac{\lambda_2\omega_2}{\lambda_1-\lambda_2}\right)\left(\lambda_1+\frac{1}{\mu}\right)k_c^*C_2(R,\tau), \tag{39}$$

where

$$S_i(R,\tau)=\sum_{k=1}^{\infty}R^{k-1}\sin(\omega_ik\tau)=\frac{\sin(\omega_i\tau)}{1+R^2-2R\cos(\omega_i\tau)},\quad i=1,2 \tag{40}$$

$$C_i(R,\tau)=\sum_{k=1}^{\infty}R^{k-1}\cos(\omega_ik\tau)=\frac{\cos(\omega_i\tau)-R}{1+R^2-2R\cos(\omega_i\tau)},\quad i=1,2 \tag{41}$$

The amplitude Eqs. (36) and (37) can be finally recast in the following compact form:

$$\frac{dA}{dt}=F_1(A,B)=p_1A+p_2A^3+p_3AB^2, \tag{42}$$

$$\frac{dB}{dt}=F_2(A,B)=p_4B+p_5B^3+p_6BA^2, \tag{43}$$

where

$$p_1=\frac{1}{2}\frac{\left(\alpha\lambda_2-\omega_1\lambda_1\left(\lambda_2+\frac{1}{\mu}\right)k_cS_1(R,\tau)\right)}{\lambda_1-\lambda_2},\quad p_2=\frac{3}{8}\left(\frac{\beta\omega_1^2\lambda_2}{\lambda_1-\lambda_2}\right),\quad p_3=\frac{3}{4}\left(\frac{\beta\omega_2^2\lambda_2}{\lambda_1-\lambda_2}\right),$$

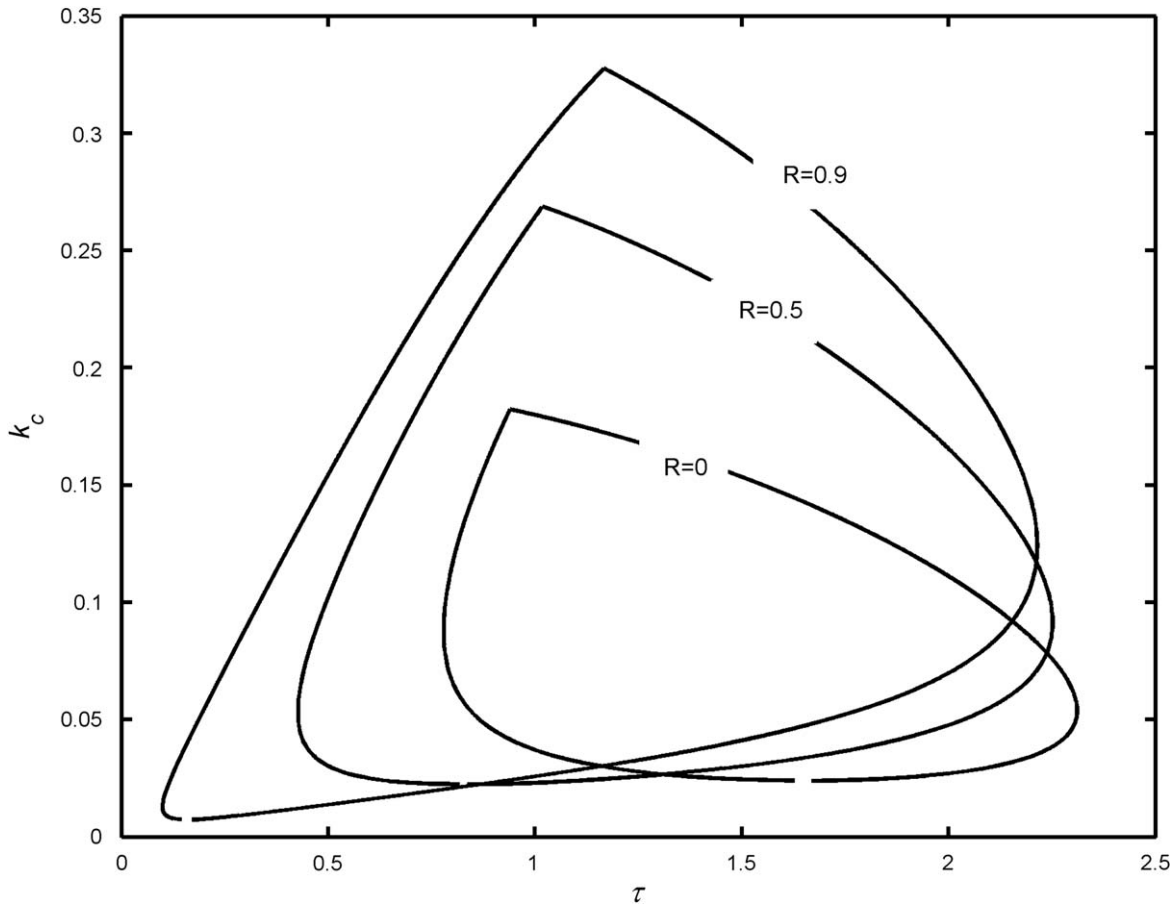

Fig. 6. Effect of recursive gain on the local stability boundary. α=0.1, μ=0.2.

Table 2
Optimum parameter values of the active device (μ=0.2, ω_a=0.9).

α	Maximum σ-stability				
	Recursive gain R=0	R=0.3	R=0.4	R=0.5	R=0.6
−0.1	−0.116 (k_c=0.1, τ=1.4)	−**0.2072** (k_c=0.11, τ=1.7)	−0.2032 (k_c=0.11, τ=1.5)	−0.2061 (k_c=0.11, τ=1.4)	−0.1868 (k_c=0.11, τ=1.3)
−0.2	−0.1131 (k_c=0.09, τ=1.95)	−0.1543 (k_c=0.1, τ=1.65)	−0.1501 (k_c=0.1, τ=1.55)	−**0.1669** (k_c=0.11, τ=1.45)	−0.1365 (k_c=0.11, τ=1.35)
−0.3	−0.0881 (k_c=0.08, τ=2)	−0.0984 (k_c=0.1, τ=1.7)	−**0.1201** (k_c=0.1, τ=1.6)	−0.1051 (k_c=0.1, τ=1.5)	−0.0868 (k_c=0.1, τ=1.4)
−0.4	−**0.0693** (k_c=0.08, τ=2.05)	−0.0578 (k_c=0.09, τ=1.75)	−0.0426 (k_c=0.09, τ=1.7)	−0.0367 (k_c=0.09, τ=1.6)	−0.0267 (k_c=0.09, τ=1.5)

Table 3
Optimum parameter values of the active device (μ=0.2, ω_a=0.85).

α	Maximum σ-stability				
	R=0	R=0.3	R=0.4	R=0.5	R=0.6
−0.1	−0.1210 (k_c=0.09, τ=2)	−**0.2305** (k_c=0.11, τ=1.9)	−0.2194 (k_c=0.11, τ=1.7)	−0.2253 (k_c=0.12, τ=1.6)	−0.2005 (k_c=0.12, τ=1.5)
−0.2	−0.1098 (k_c=0.08, τ=2.1)	−0.1678 (k_c=0.1, τ=1.9)	−**0.1766** (k_c=0.11, τ=1.75)	−0.1412 (k_c=0.11, τ=1.65)	−0.1339 (k_c=0.12, τ=1.55)
−0.3	−0.0933 (k_c=0.08, τ=2.15)	−**0.1277** (k_c=0.1, τ=1.95)	−0.0822 (k_c=0.11, τ=1.85)	−0.0987 (k_c=0.11, τ=1.75)	−0.0806 (k_c=0.11, τ=1.65)
−0.4	−**0.0481** (k_c=0.08, τ=2.2)	−0.0411 (k_c=0.1, τ=2)	−0.0294 (k_c=0.1, τ=1.9)	−0.0172 (k_c=0.11, τ=1.85)	−0.0346 (k_c=0.11, τ=1.7)

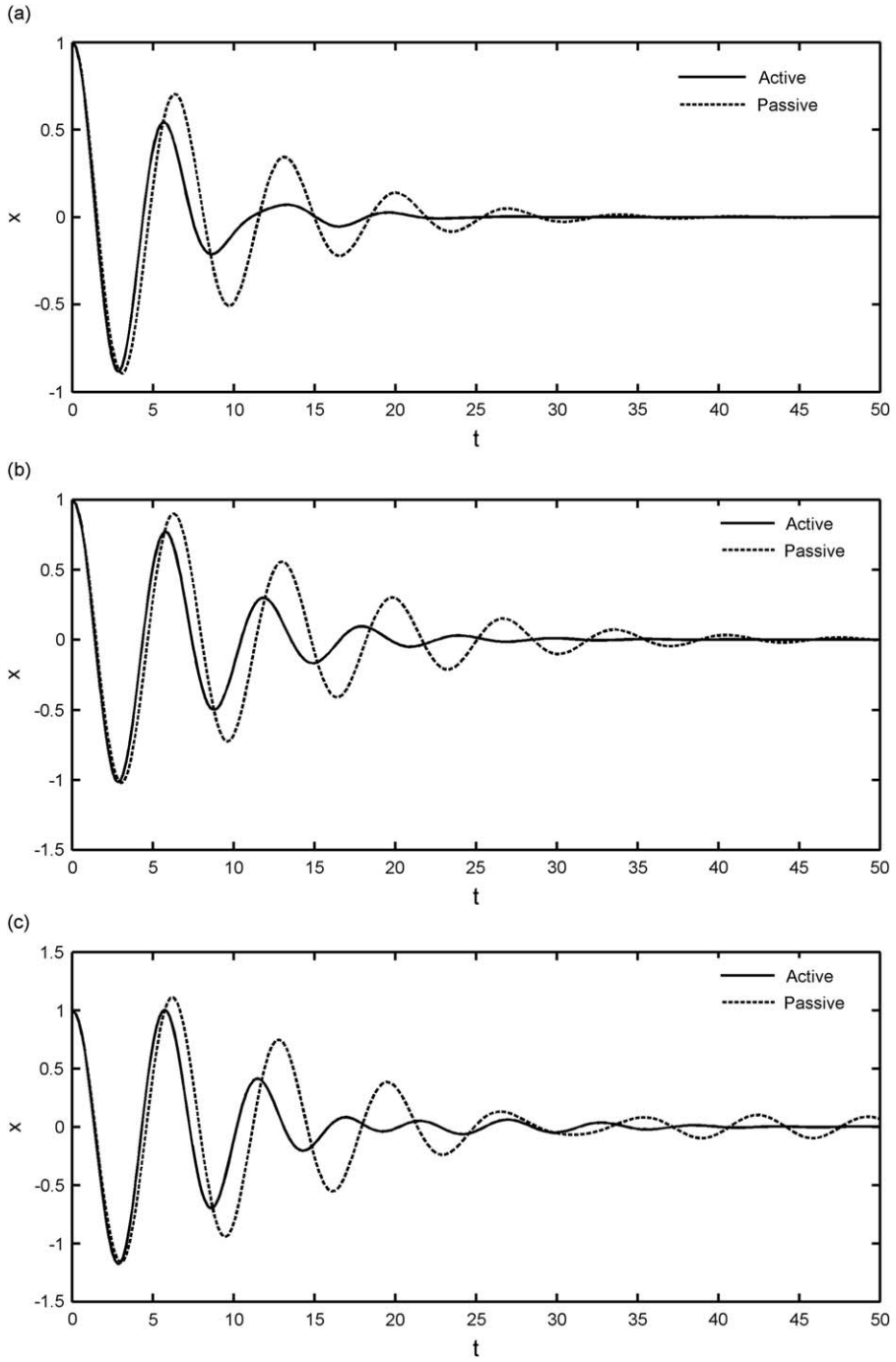

Fig. 7. (a) Time-history plots of the response of the primary system with passive and active absorber. $\alpha=-0.1$, $\beta=0.1$, $\mu=0.2$. Optimum parameter values of the passive absorber: $\omega_a=0.85$, $c=0.12$. Optimum parameter values of the active device: $\omega_a=0.85$, $R=0.3$, $\tau=1.9$, $k_c=0.11$. (b) Time-history plots of the response of the primary system with passive and active absorber. $\alpha=-0.2$, $\beta=0.1$, $\mu=0.2$. Optimum parameter values of the passive absorber: $\omega_a=0.87$, $c=0.11$. Parameter values of the active device: $\omega_a=0.85$, $R=0.4$, $\tau=1.75$, $k_c=0.11$. (c) Time-history plots of the response of the primary system with passive and active absorber. $\alpha=-0.3$, $\beta=0.1$, $\mu=0.2$. Optimum parameter values of the passive absorber: $\omega_a=0.89$, $c=0.09$. Parameter values of the active device: $\omega_a=0.85$, $R=0.3$, $\tau=1.95$, $k_c=0.1$.

$$p_4=\frac{1}{2}\frac{\left(-\alpha\lambda_1+\omega_2\lambda_2\left(\lambda_1+\frac{1}{\mu}\right)k_cS_2(R,\tau)\right)}{\lambda_1-\lambda_2},\quad p_5=-\frac{3}{8}\left(\frac{\beta\omega_2^2\lambda_1}{\lambda_1-\lambda_2}\right),\quad p_6=-\frac{3}{4}\left(\frac{\beta\omega_1^2\lambda_1}{\lambda_1-\lambda_2}\right).$$

The steady-state solutions (equilibrium points in the A–B phase plane) of Eqs. (42) and (43) can be obtained by solving the following nonlinear algebraic equations:

$$p_1 A + p_2 A^3 + p_3 A B^2 = 0, \tag{44}$$

$$p_4 B + p_5 B^3 + p_6 B A^2 = 0. \tag{45}$$

Four different steady-state solutions are possible as listed below

(1) $A=0$, $B=0$ (static equilibrium),
(2) $A=0$, $B=\sqrt{-p_4/p_5}$ (oscillation at the second mode),
(3) $A=\sqrt{-p_1/p_2}$, $B=0$ (oscillation at the first mode)
(4) $A=\sqrt{p_3p_4-p_1p_5/p_2p_5-p_3p_6}$, $B=\sqrt{p_1p_6-p_2p_4/p_2p_5-p_3p_6}$ (dual mode oscillation: both the modes are present in the oscillation).

Stabilities of these four different solutions are ascertained by computing the eigenvalues of the Jacobian of the flow of Eqs. (42) and (43) at the equilibrium points. The expression of the Jacobian is given below

$$J = \begin{bmatrix} p_1 + 3p_2A^2 + p_3B^2 & 2p_3AB \\ 2p_6AB & p_4 + 3p_5B^2 + p_6A^2 \end{bmatrix}. \tag{46}$$

It may be observed from the expression of the Jacobian (46) that the local stability of the trivial static equilibrium ($A=0$ and $B=0$) is determined by the signs of p_1 and p_4. The trivial equilibrium is stable if $p_1<0$ and $p_4<0$. The degree of stability is also given by the magnitudes of p_1 and p_4.The variations of p_1 and p_4 with the time-delay for different values of R are depicted in Figs. 8(a) and (b). With the increasing value of the recursive gain R, both p_1 and p_4 apparently become *more negative* within a range (smaller values of time-delay) of time-delays. This implies that the recursive gain can improve the degree of stability. This explains the improvement of the σ-stability with the higher recursive gain observed in Section 5. However, the present analysis is valid only for small values of the feedback gain.

Figs. 9(a) and (b) illustrate the typical variations of the amplitude of vibration (modal) with the time-delay. The dual mode oscillations are always found unstable and hence omitted in the plots. The analytical results are found to be in close agreement with that of numerical simulations. It may be observed that appropriate selections of the recursive gain and the time-delay can completely quench the self-excited vibration (Fig. 9(b)). Even when complete stabilization of the trivial equilibrium is not achieved, judicious selection of the time-delay can significantly reduce the amplitude of oscillation. Variations of the amplitude of oscillations with the absorber frequency are shown in Fig. 10. It is apparent from Fig. 10 that the appropriate selections of the gains and the time-delay render the system robust against absorber mistuning (up to a certain limit).

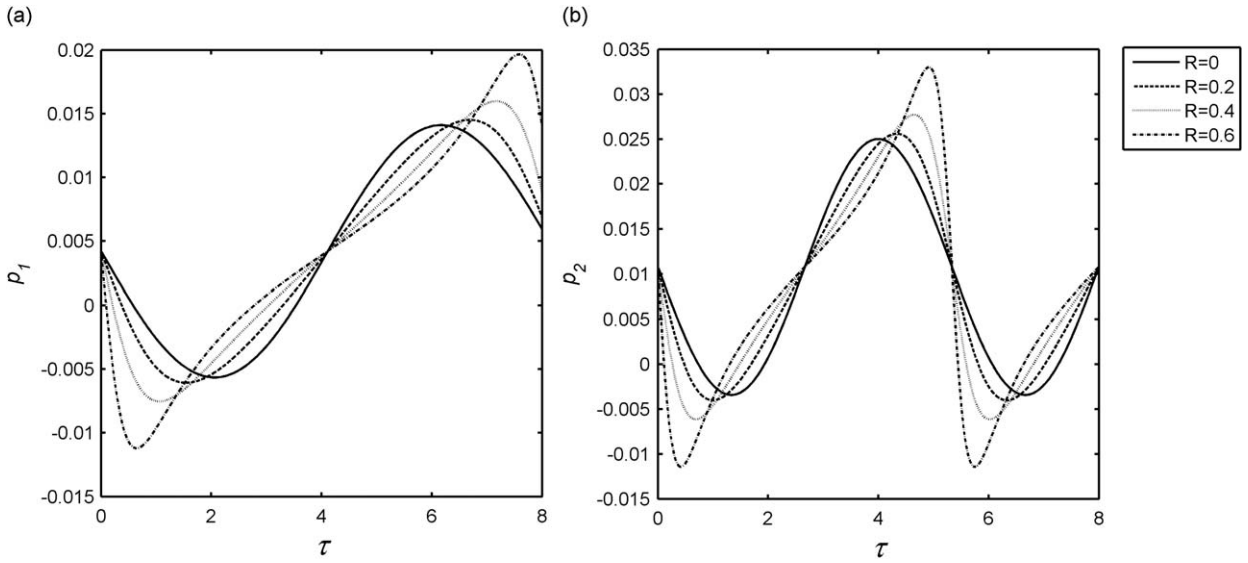

Fig. 8. Variations of p_1 and p_4 with time-delay. $\alpha=-0.03$, $\beta=0.03$, $\mu=0.2$, $\omega_a=0.9$, $k_c=0.01$.

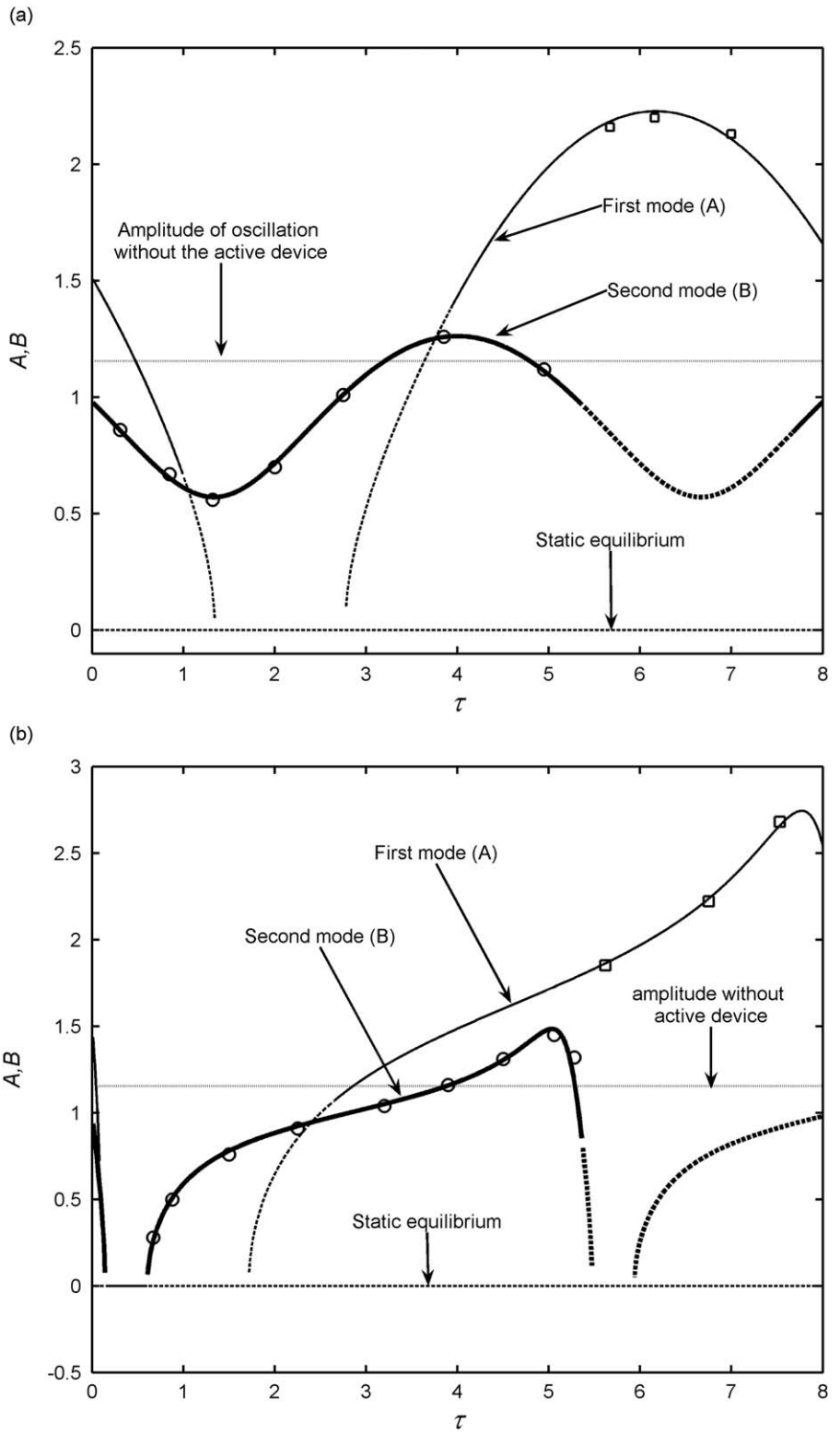

Fig. 9. (a) Variations of the amplitude with time-delay. μ=0.2, ω_a=0.9, α=−0.03, β=0.03, k_c=0.005, R=0. *o*, numerical simulations (second modes); □, numerical simulations (first mode). Solid curves—stable; dashed curves—unstable. (b) Variations of the amplitude with time-delay. μ=0.2, ω_a=0.9, α=−0.03, β=0.03, k_c=0.005, R=0.7. *o*, numerical simulations (second mode); □, numerical simulations (first mode). Solid curves—stable; dashed curves—unstable.

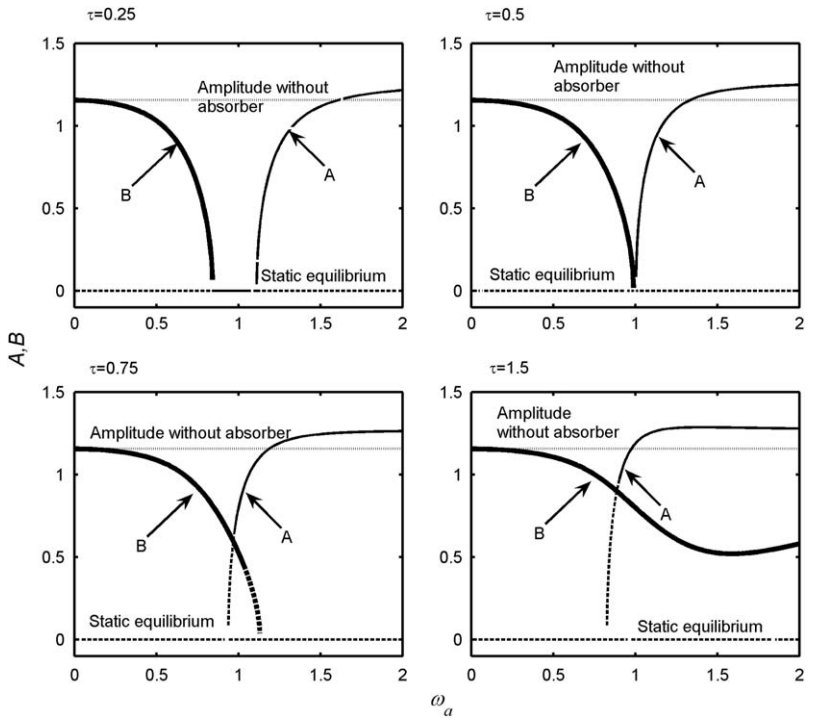

Fig. 10. Variations of the amplitude with absorber frequency. μ=0.2, α=−0.1, β=0.1, k_c=0.01, R=0.9. Solid curves—stable; dashed curves—unstable.

7. Conclusions

The present paper analyses the efficacy of an inertial, active device in controlling the self-excited oscillation of a single degree-of-freedom Rayleigh oscillator. The proposed active absorber is a standalone system comprising of a spring suspended mass and an actuator controlled by the generalized, time-delayed feedback of the acceleration of the absorber mass itself. As the absorber runs on its internal feedback and does not require any external sensory input, the device operates when simply attached to the self-excited system. This renders the strategy very much user friendly. The control algorithm is recursive in nature and utilizes a large amount of information regarding the past history of the dynamics. Both the linear and nonlinear analyses have shown that the three control parameters, namely the control gain, recursive gain and the time-delay can be appropriately chosen to quench the self-excited oscillation. A proper selection of the control parameters can significantly reduce the amplitude of vibration when complete quenching is not possible.

The performance of the proposed device is compared with that of a passive DVA. Like a passive absorber, the active device can control only a certain level of the instability inherent in the self-excited system. However, the proposed device is shown to offer better stability conditions compared to a passive DVA.

References

[1] W.M. Mansour, Quenching of limit cycles of a van der Pol oscillator, *Journal of Sound and Vibration* 25 (1972) 395–405.
[2] A. Tondl, Quenching of self-excited vibrations; equilibrium aspects, *Journal of Sound and Vibration* 42 (1975) 251–260.
[3] K.R. Asfar, Quenching of self-excited vibrations, *Transactions of the American Society of Mechanical Engineers, Journal of Vibration, Acoustic, Stress, and Reliability in Design* 111 (1989) 130–133.
[4] S. Chatterjee, A.K. Mallik, A. Ghosh, Impact dampers for controlling self-excited oscillation, *Journal of Sound and Vibration* 193 (5) (1996) 1003–1014.
[5] A. Tondl, T. Ruigrok, F. Verhulst, R. Nabergoj, *Autoparametric Resonance in Mechanical Systems*, Cambridge University Press, Cambridge, New York, 2000.
[6] B.D. Hall, D.T. Mook, A.H. Nayfeh, S. Preidikman, Novel strategy for suppressing the flutter oscillations of aircraft wings, *AIAA Journal* 39 (2001) 1843–1850.
[7] A.A. El-Badawy, T.N. Nasar El-Deen, Quadratic nonlinear control of a self-excited oscillator, *Journal of Vibration and Control* 13 (4) (2007) 403–414.
[8] A. Tondl, On the interaction between self-excited and parametric vibrations, *National Research Institute for Machine Design, Prague, Monographs and Memoranda* 25 (1978).
[9] A. Tondl, To the problem of quenching self-excited vibrations, *Acta Technica CSAV* 43 (1998) 109–116.
[10] S. Fatimah, F. Verhulst, Suppressing flow-induced vibrations by parametric excitation, *Nonlinear Dynamics* 23 (2003) 275–297.
[11] H. Ecker, A parametric absorber for friction-induced vibrations, *Proceedings of ASME Design Engineering Technical Conference*, Chicago, IL, DETC2003/VIB-48474 (2003).
[12] K. Makihara, H. Ecker, F. Dohnal, Stability analysis of open-loop stiffness control to suppress self-excited vibrations, *Journal of Vibration and Control* 11 (2005) 643–669.
[13] F. Dohnal, Suppressing self-excited vibrations by synchronous stiffness and damping variation, *Journal of Sound and Vibration* 306 (2007) 136–152.

[14] F. Dohnal, Optimal dynamic stabilization of a linear system by periodic stiffness excitation, *Journal of Sound and Vibration* 320 (2009) 777–792.
[15] F. Dohnal, A. Tondl, Suppressing flutter vibrations by parametric inertia excitations, *Transactions of ASME, Journal of Applied Mechanics* 76 (2009) 031006-1.
[16] S. Chatterjee, On the principle of impulse damper: a concept derived from impact damper, *Journal of Sound and Vibration* 312 (2008) 584–605.
[17] B. Armstrong-Hélouvry, P. Dupont, C. Canudas de Wit, A survey of models, analysis tools and compensation methods for the control of machines with friction, *Automatica* 30 (7) (1994) 1083–1138.
[18] M.A. Heckl, D. Abrahams, Active control of friction driven oscillations, *Journal of Sound and Vibration* 193 (1) (1996) 417–426.
[19] K. Popp, M. Rudolph, Vibration control to avoid stick-slip motion, *Journal of Vibration and Control* 10 (2004) 1585–1600.
[20] J.J. Thomsen, Using fast vibrations to quench friction-induced oscillations, *Journal of Sound and Vibration* 228 (5) (1999) 1079–1102.
[21] S. Chatterjee, T.K. Singha, S.K. Karmakar, Effect of high-frequency excitation on a class of mechanical systems with dynamic friction, *Journal of Sound and Vibration* 269 (2004) 61–89.
[22] S. Chatterjee, Non-linear control of friction-induced self-excited vibration, *International Journal of Nonlinear Mechanics* 42 (3) (2007) 459–469.
[23] S. Chatterjee, On the design criteria of dynamic vibration absorbers for controlling friction-induced oscillations, *Journal of Vibration and Control* 14 (3) (2008) 397–415.
[24] F.M. Atay, van der Pol's oscillator under delayed feedback, *Journal of Sound and Vibration* 218 (2) (1998) 333–339.
[25] F.M. Atay, Delayed feedback control of oscillations in nonlinear planar systems, *International Journal of Control* 75 (2002) 297–304.
[26] A. Maccari, Vibration control of parametrically excited Lienard system, *International Journal of Nonlinear Mechanics* 41 (2006) 146–155.
[27] A. Maccari, Vibration control for the primary resonance of the van der Pol oscillator by a time delay state feedback, *International Journal of Nonlinear Mechanics* 38 (2003) 123–131.
[28] X. Li, J.C. Ji, C.H. Hansen, C. Tan, Response of a Duffing-Van der Pol oscillator under delayed feedback control, *Journal of Sound and Vibration* 291 (2006) 644–655.
[29] F.-J. Elmer, Controlling friction, *Physical Review E* 57 (1998) 4903–4906.
[30] J. Das, A.K. Mallik, Control of friction driven oscillation by time-delayed state feedback, *Journal of Sound and Vibration* 297 (3–5) (2006) 578–594.
[31] S. Chatterjee, Time-delayed feedback control of friction-induced instability, *International Journal of Nonlinear Mechanics* 42 (2007) 1127–1143.
[32] S. Chatterjee, P. Mahata, Time-delayed absorber for controlling friction-induced self-excited oscillation, *Journal of Sound and Vibration* 322 (2009) 39–59.
[33] S. Chatterjee, Vibration control by recursive time-delayed acceleration feedback, *Journal of Sound and Vibration* 317 (1–2) (2008) 67–90.
[34] M.A. Cruz, J.K. Hale, Stability of functional differential equations of neutral type, *Journal of Differential Equations* 7 (1970) 334–355.
[35] T. Vyhlídal, P. Zítek, Quasipolynomial mapping based rootfinder for analysis of time delay systems, *Proceedings of IFAC Workshop on Time-Delay Systems*, TDS'03, Rocquencourt, 2003.